https://doi.org/10.18321/ectj1559

Promising Directions in Chemical Processing of Methane from Coal Industry. Part 3. Catalytic Tests

E.V. Matus*, M.A. Kerzhentsev, A.P. Nikitin, S.A. Sozinov, Z.R. Ismagilov

Federal Research Center of Coal and Coal Chemistry, Siberian Branch, RAS,
18, pr. Sovetskiy, Kemerovo, Russia

Article info

Received:
20 October 2023

Received in revised form:
25 December 2023

Accepted:
15 February 2024

Keywords:
Coal mine methane
Tri-reforming of methane
Ni-based catalyst
Hydrogen production

Abstract

For the processing of coal mine methane into hydrogen-containing gas, a catalytic process of methane tri-reforming ($CH_4 + O_2 + CO_2 + H_2O$) was proposed and its component reactions were studied – partial oxidation ($CH_4 + O_2$, POM), dry reforming ($CH_4 + CO_2$, DRM) and steam reforming ($CH_4 + H_2O$, SRM) of methane. Promoted nickel supported on aluminum oxide was used as a catalyst. Experiments were carried out by varying temperature (600–850 °C), contact time (0.04–0.15 s), linear feed rate (40–240 cm/min) and composition of the reaction mixture (POM – $CH_4 : O_2 : He = 1 : (0.5–0.7) : (3.3–3.4)$; DRM – $CH_4 : CO_2 : He = 1 : (0.8–1.4) : (2.6–3.2)$; SRM – $CH_4 : H_2O : He = 1 : (0.8–2.0) : (2.0–3.2)$). Optimal reaction conditions were determined to ensure maximum efficiency of hydrogen production by reforming methane-containing mixtures of various compositions (temperature in the range of 800–850 °C, contact time 0.15 s, linear feed rate 160 cm/min, molar ratio of $CH_4 : O_2 = 1 : 0.5$ for POM, $CH_4 : CO_2 = 1 : 1$ for DRM and $CH_4 : H_2O = 1 : 1.1$ for SRM). The degree of catalyst carbonization during the reactions was reduced (from 3 to 1.5% for POM, from 20.7 to 2.2% for DRM, and from 15.2 to 0.4% for SRM) due to an increase in the O/C molar ratio in the initial reaction mixture. Regulation of H_2/CO molar ratio was achieved over a wide range (0.9–6.5). It has been shown that the hydrogen concentration in the resulting hydrogen-containing mixture is determined by the type of process and is equal to 30±5 vol.%.

1. Introduction

The coal industry is a key link in the global fuel and energy system. Over the past two decades, the share of coal in global primary energy has been 25–30% [1]. From 2012 to 2022, total world coal production increased from 8188.0 to 8803.4 million tons. In terms of production volume (Fig. 1a), China ranks first (4560 million tons), the Russian Federation is sixth (439 million tons) and Kazakhstan is ninth (118 million tons). According to Wood Mackenzie experts [2], despite government pledges and investments in renewable energy, coal remains difficult to replace in terms of electricity reliability. As a result, coal production is expected to continue to grow in Asia in the near-term, particularly in India and Southeast Asia.

Coal remains one of the most in-demand energy resources and is of great importance in the global energy market. According to the Energy Institute Statistical Review of World Energy [1], coal prices reached record levels in 2022, with European prices averaging $294/tonne and the Japan CIF spot price averaging $225/tonne (increases of 145% and 45% over 2021 respectively). The leadership in the consumption of this resource is held by China by a wide margin; the top three also include India and the USA (Fig. 1b).

*Corresponding author.
E-mail address: matus_e@mail.ru

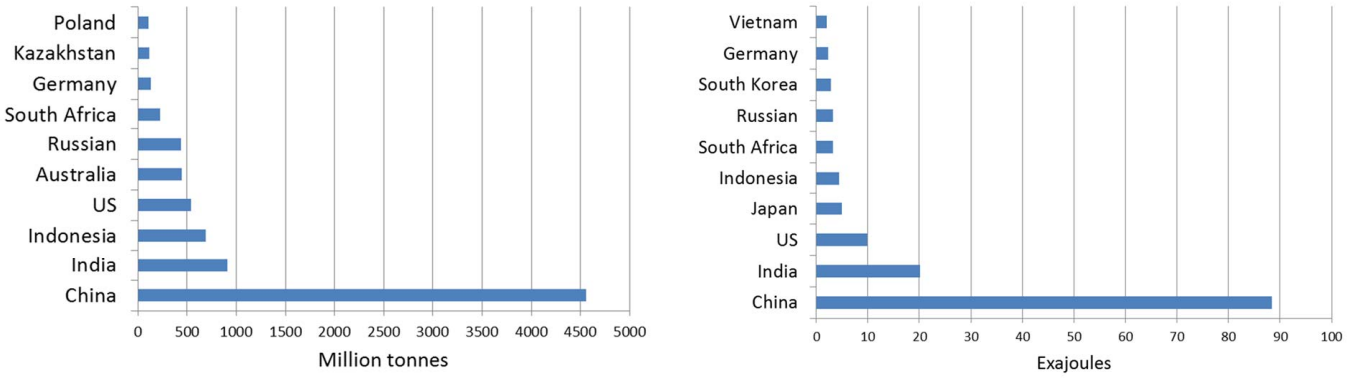

Fig. 1. Coal production (a) and consumption (b) by country. According to data for 2022 from [1].

Activities associated with coal mining (underground mining, surface mining, and post-mining) are responsible for large amounts of CH_4 emissions into the atmosphere. Total methane emissions from the coal industry in 2022 amounted to 41.8 million tons, which is equal to almost 30% of anthropogenic methane emissions [3]. Figure 2 demonstrates coal mine methane emissions and methane intensity of production in selected countries. Unsurprisingly, the main coal-producing countries are also the main emitters of methane from the coal industry. Methane emissions from coal mining are divided into thermal coal (mainly used for electricity generation) and coking coal (mainly for industrial use). Since the volume of thermal coal production is much higher than coking coal (87 vs. 13%) [4], methane emissions come mostly from steam coal and lignite (Fig. 2). Significant fluctuations in the intensity of methane emission are connected with different conditions of occurrence and, as a consequence, different methane content of coal seams. The Intergovernmental Panel on Climate Change (IPCC) proposes different methane emission factors per tonne of coal mined depending on the depth and mining method [5]. Emission factors for underground mining are 10 m^3/t – for mining depths of less than 200 m, 18 m^3/t – for depths from 200 to 400 m, 25 m^3/t – for mines with a depth of more than 400 m, and for surface mining by order of magnitude less: 0.3 m^3/t – for development depths less than 25 m, 1.2 m^3/t – for depths from 20 to 50 m, 2.0 m^3/t – for areas more than 50 m deep. Because the presence of methane in the atmosphere degrades air quality and contributes to global warming, efforts are being made to reduce methane emissions from coal mines [6].

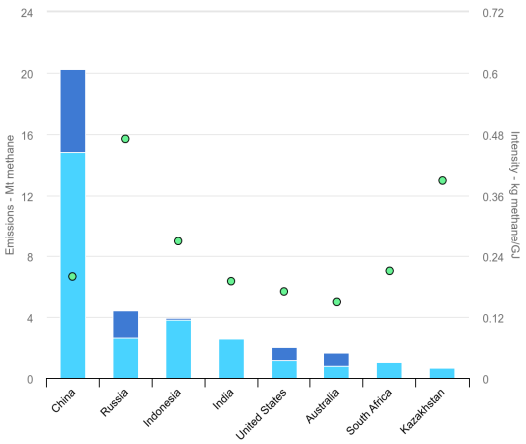

Fig. 2. Coal mine methane emissions and methane intensity of production in selected countries [7].

One of the ways to utilize coal mine methane is its chemical processing using catalytic technologies [8–13]. A promising process for processing coal mine methane is the tri-reforming of methane (reaction 1), for which the change in the enthalpy of the reaction ($\Delta_r H_o T$) and the change in the Gibbs free energy of the reaction ($\Delta_r G_o T$) at 800 °C and 1 bar are +154 kJ/mol and –108 kJ/mol, respectively. Thermodynamic analysis of this reaction showed that at 800 °C the conversion of methane is 94%, the yield of hydrogen is 91%, and the concentration of hydrogen is 61% [14].

$$3CH_4 + 0.5O_2 + H_2O + CO_2 \rightarrow 4CO + 7H_2 \quad (1)$$

This reaction is a combination of three main reactions – partial oxidation (POM, reaction 2), dry reforming (DRM, reaction 3) and steam reforming (SRM, reaction 4) of methane:

$$CH_4 + 0.5O_2 \leftrightarrow CO + 2H_2 \quad (2)$$

$$CH_4 + CO_2 \leftrightarrow 2CO + 2H_2 \quad (3)$$

$$CH_4 + H_2O \leftrightarrow CO + 3H_2 \quad (4)$$

The tri-reforming process is designed to convert methane into synthesis gas, which can then be used to produce hydrogen, methanol, and ammonia [15]. It is noteworthy that oxygen, water, and carbon dioxide can act as oxidizing reagents. Accordingly, if we have a wet methane-air gas mixture from the mine's degassing system, we can use it as is or by adding carbon dioxide to it. This ensures flexibility of the process and ease of regulation of the resulting molar ratio of reaction products, in particular, H_2/CO. The reaction conditions also impose certain requirements on tri-reforming catalyst: the catalyst must be active towards all reagents and resistant to re-oxidation, formation of carbon deposits, and sintering. And, most importantly, it must maintain its activity despite wide changes in the initial reaction mixture over time. Based on previous studies, we proposed multi-component catalysts containing aluminum, cerium, and nickel oxides – $Ce_{0.2}Ni_{0.8}O_{1.2}$/Al_2O_3 [16]. In such material, aluminum oxide provides the thermal stability of the catalyst; cerium dioxide serves as an oxygen buffer and plays a role in the activation of oxygen-containing molecules, while metal nickel is highly active towards methane activation [17].

Thus, in this work, in continuation of our research on the chemical processing of methane from the coal industry [14, 16], the reactions that make up the tri-reforming process were studied – partial oxidation, dry reforming, and steam reforming of methane in the presence of a $Ce_{0.2}Ni_{0.8}O_{1.2}/Al_2O_3$ catalyst and with a wide variation of reaction conditions.

2. Experimental

2.1. Catalyst preparation

The $Ce_{0.2}Ni_{0.8}O_{1.2}/Al_2O_3$ catalyst was prepared by the citrate sol-gel method according to the previously described procedure [16]. Spherical Al_2O_3 with a grain size of 0.3–0.8 mm was impregnated with an aqueous solution containing $Ce(NO_3)_3{\cdot}6H_2O$, $Ni(NO_3)_2{\cdot}6H_2O$ and $C_6H_8O_7$. After that, the sample was dried at 90 °C, followed by calcination in air at 500 °C for 4 h and activation in 30 vol.% H_2/70 vol.% Ar at 800 °C for 1 h. The characteristics of the fresh and activated $Ce_{0.2}Ni_{0.8}O_{1.2}/Al_2O_3$ catalysts are given in [16].

2.2. Catalyst testing

The catalyst testing was carried out in a flow quartz reactor (internal diameter 11 mm) at atmospheric pressure with varying temperature (600–850 °C), contact time (0.04–0.15 s), linear feed rate (40–240 cm/min) and composition of the reaction mixture (POM – CH_4:O_2:He = 1:(0.5–0.7):(3.3–3.4); DRM – CH_4:CO_2:He = 1:(0.8–1.4):(2.6–3.2); SRM – CH_4:H_2O:He = 1:(0.8–2.0):(2.0–3.2)) in the presence of a $Ce_{0.2}Ni_{0.8}O_{1.2}/Al_2O_3$ catalyst. The tests were performed in the stepwise temperature rise mode 600 → 850 °C. The heating rate was 10 degrees per minute; the holding time at each temperature was 40 minutes.

The composition of the reaction mixture was analyzed by gas chromatography on a Kristall 2000M chromatograph. The separation of H_2, He, CO, CO_2, and CH_4 was carried out on a steel packed column 2 m long, 3 mm in diameter with SKT carbon (thermal conductivity detector, carrier gas – Ar, flow – 30 ml/min, temperature 165 °C). The following reaction indicators were calculated:

CH_4 conversion, %: $X_{CH_4} = 100 \times \left(F^{in}_{CH_4} - F^{out}_{CH_4}\right) / F^{in}_{CH_4}$,

H_2 yield, %: $Y_{H_2} = 100 \times F^{out}_{H_2} / \left(2F^{in}_{CH_4} + F^{in}_{H_2O}\right)$,

CO yield, %: $Y_{CO} = 100 \times F^{out}_{CO} / \left(F^{in}_{CH_4} + F^{in}_{CO_2}\right)$,

CO_2 conversion, %: $X_{CO_2} = 100 \times \left(F^{in}_{CO_2} - F^{out}_{CO_2}\right) / F^{in}_{CO_2}$ (for DRM reaction),

CO_2 yield, %: $Y_{CO_2} = 100 \times F^{out}_{CO_2} / F^{in}_{CH_4}$ (for POM and SRM reactions),

where F_i is the molar flow rate of the reagent (i) at the inlet (in) and outlet (out) of the reactor.

2.3. Catalyst characterizations

Thermal analysis (differential thermal analysis (DTA), thermogravimetric analysis (TGA) and differential thermogravimetric analysis (DTG)) of the catalysts after testing in POM, DRM and SRM reactions in the stepwise temperature rise mode 600 → 850 °C were carried out on a NETZSCH STA 449 C thermal analyzer (NETZSCH-Geratebau GmbH, Germany) in the temperature range of 25–900 °C with a temperature increase rate of 10 °C/min, in air.

3. Results and discussion

3.1. Partial oxidation of methane

For POM it was revealed that an increase in temperature has a positive effect on the efficiency of the process in the temperature range of 600–850 °C (Table 1, Fig. 3).

Table 1. The influence of temperature, contact time, linear feed rate and composition of the reaction mixture on the performance of the POM reaction

Catalyst quantity, g	Contact time, s	Linear feed rate, cm/min	Temperature of reaction, °C	Reaction indicators				
				X_{CH4}	Y_{CO2}	Y_{H2}	Y_{CO}	H_2/CO
$CH_4 : O_2 : He = 1 : 0.6 : 3.4$								
0.125	0.04	160	600	78	22	74	52	2.8
			700	92	14	90	72	2.5
			800	97	10	97	81	2.4
0.250	0.08	160	600	70	20	65	46	2.8
			700	84	14	75	62	2.4
			800	89	11	84	70	2.4
0.500	0.15	160	600	74	19	74	52	2.9
			700	92	10	90	75	2.4
			800	98	6	96	84	2.3
0.125	0.15	40	600	63	13	70	49	2.8
			700	82	3	92	76	2.4
			800	90	0	95	83	2.3
0.250	0.15	80	600	72	20	68	47	2.9
			700	92	10	96	77	2.5
			800	98	6	96	84	2.3
0.750	0.15	240	600	65	18	64	47	2.7
			700	84	9	83	69	2.4
			800	93	5	92	81	2.2
$CH_4 : O_2 : He = 1 : 0.5 : 3.5$								
0.500	0.15	160	600	68	15	70	49	2.9
			700	85	5	86	72	2.4
			800	94	0	96	84	2.3
$CH_4 : O_2 : He = 1 : 0.7 : 3.3$								
0.500	0.15	160	600	80	28	75	49	3.0
			700	93	18	86	68	2.5
			800	97	14	92	76	2.4

With increasing temperature from 600 to 800 °C, the process parameters increase (X_{CH4}: 68→94%, Y_{H2}: 70→96%, Y_{CO}: 49→84%), and at a reaction temperature of 850 °C they are close to equilibrium (Fig. 3). In this case, a decrease in the H_2/CO ratio (2.9→2.3) and the yield of CO_2 byproduct (15→0) is observed.

Changing the contact time (0.04–0.15 s) and the linear feed rate of the reaction mixture (40–240 cm/min) has little effect on the performance of the process (Table 1). At a contact time of 0.15 s, a minimum CO_2 yield is achieved, which may indicate its conversion with methane into synthesis gas at a sufficiently long contact time. It has been established that an increase in the CH_4/O_2 ratio from 1.4 to 2.0 leads to a slight decrease in methane conversion and an increase in the yield of target reaction products (Fig. 3, Table 1), a sharp decrease in the yield of CO_2 (15→3%) due to a decrease in the contribution of the side reaction deep oxidation of methane, which is consistent with modern ideas about the mechanism of reforming and methane oxidation reactions [15].

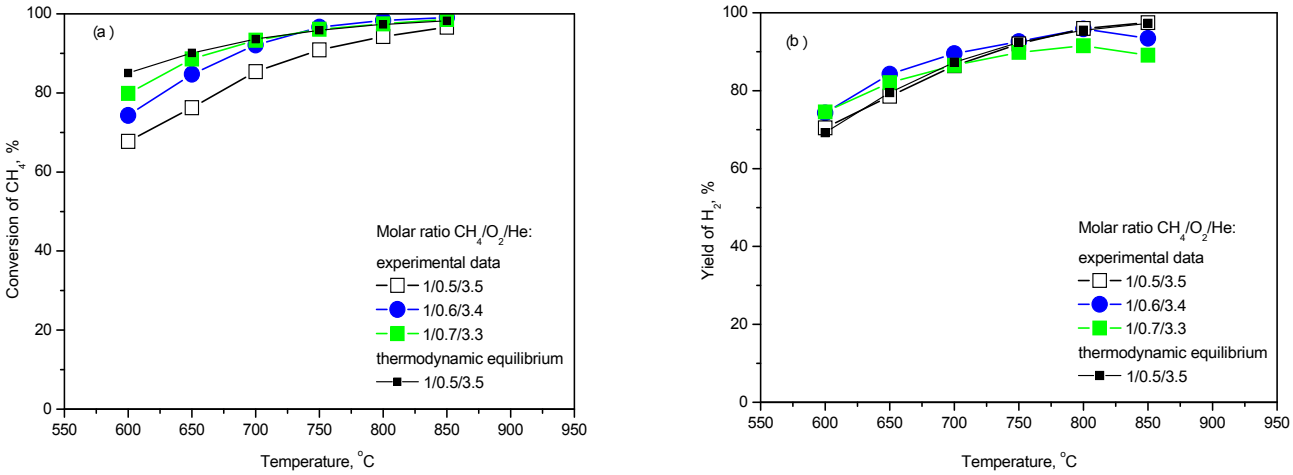

Fig. 3. Temperature dependence of methane conversion (a) and hydrogen yield (b) in the POM reaction at different molar ratios of reagents.

3.2. Dry reforming of methane

It has been established that for DRM, the reaction rates in the temperature range of 600–800 °C are lower than the values calculated for thermodynamic equilibrium conditions (Table 2, Fig. 3), which indicates kinetic control of the reaction. With an increase in the reaction temperature from 600 to 800 °C, the process indicators increase (X_{CH4}: 45→96%, X_{CO2}: 50→92%, Y_{H2}: 48→97%, Y_{CO}: 51→94%) and at a reaction temperature of 850 °C are close to equilibrium (Fig. 4). The values of the H_2/CO molar ratio weakly depend on the process temperature and are equal to ~1.0 (Table 2). Increasing the contact time from 0.04 to 0.15 s leads to improved process performance (X_{CH4}: 71→97%, X_{CO2}: 66→81%, Y_{H2}: 69→95%, Y_{CO}: 69→91%). Changing the linear feed rate of the reaction mixture in the range of 40–240 cm/min has little effect on the performance of the process, which indicates the absence of external diffusion (Table 2).

When varying the composition of the reaction mixture, a change is observed in both the conversion of reagents and the yield of target reaction products (Table 2, Fig. 4). A decrease in the CH_4/CO_2 molar ratio in the reaction mixture from 1.3 to 0.7 leads to an increase in CH_4 conversion (87→98%), a decrease in CO_2 conversion (96→87%) and a decrease in the H_2/CO molar ratio (1.1→1.0) in the reaction products. The yield values of the reaction products have a nonlinear relationship: the maximum values are achieved at CH_4/CO_2 = 1.0 (Y_{H2} = 97%, Y_{CO} = 94%), at which high conversion is observed for both reagents (X_{CH4} = 96%, X_{CO2} = 92%), as well as a small contribution of side reactions – the reverse reaction of CO conversion with water vapor (reaction 5), which occurs at low values CH_4/CO_2; methane cracking (reaction 6), which occurs at high CH_4/CO_2 values and is the cause of a high degree of carbonation.

$$H_2 + CO_2 \leftrightarrow CO + H_2O \quad (5)$$

$$CH_4 \leftrightarrow C + 2H_2 \quad (6)$$

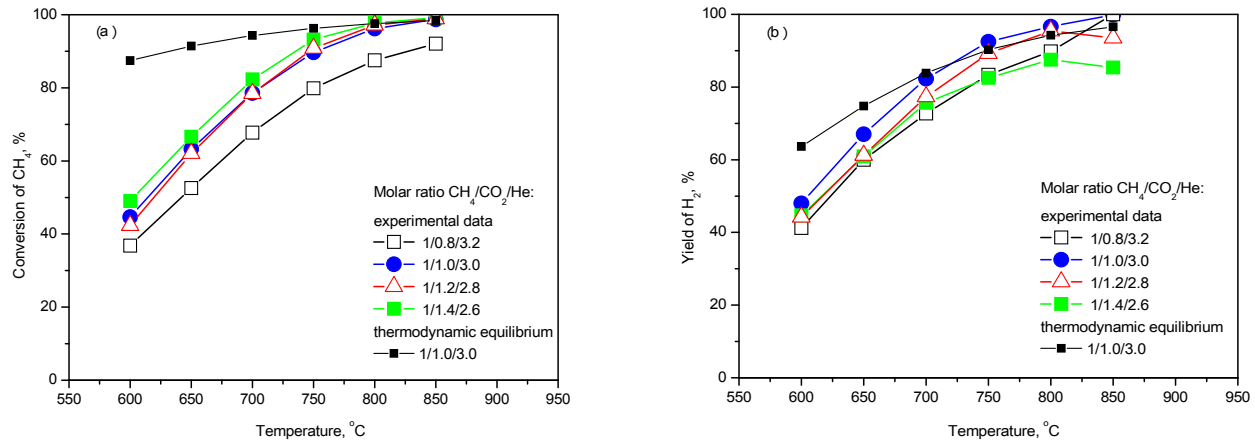

Fig. 4. Temperature dependence of methane conversion (a) and hydrogen yield (b) in the DRM reaction at different molar ratios of reagents.

Table 2. The influence of temperature, contact time, linear feed rate and composition of the reaction mixture on the performance of the DRM reaction

Catalyst quantity, g	Contact time, s	Linear feed rate, cm/min	Temperature of reaction, °C	Reaction indicators				
				X_{CH4}	Y_{CO2}	Y_{H2}	Y_{CO}	H_2/CO
$CH_4 : CO_2 : He = 1 : 1.2 : 2.8$								
0.125	0.04	160	600	27	29	34	35	0.9
			700	54	52	52	54	0.9
			800	71	66	69	69	0.9
0.250	0.08	160	600	30	32	36	37	1.0
			700	58	57	60	60	1.0
			800	72	69	71	71	1.0
0.500	0.15	160	600	42	40	44	45	0.9
			700	78	68	77	75	0.9
			800	97	81	95	91	0.9
0.125	0.15	40	600	58	51	57	57	0.9
			700	91	75	85	81	0.9
			800	99	82	92	87	1.0
0.250	0.15	80	600	44	43	45	44	0.9
			700	80	74	79	74	1.0
			800	96	85	88	83	1.0
0.750	0.15	240	600	44	40	45	45	0.9
			700	79	66	82	76	0.9
			800	98	80	91	88	0.9
$CH_4 : CO_2 : He = 1 : 0.8 : 3.2$								
0.500	0.15	160	600	37	46	41	43	1.1
			700	68	78	73	73	1.1
			800	87	96	90	90	1.1
$CH_4 : CO_2 : He = 1 : 1.0 : 3.0$								
0.500	0.15	160	600	45	50	48	51	0.9
			700	79	80	82	81	1.0
			800	96	92	97	94	1.0
$CH_4 : CO_2 : He = 1 : 1.4 : 2.6$								
0.500	0.15	160	600	49	54	45	44	0.9
			700	82	76	76	70	1.0
			800	98	87	87	80	1.0

3.3. Steam reforming of methane

For the SRM, it was revealed that an increase in temperature has a positive effect on the efficiency of the process on the catalyst under study in the temperature range of 600–850 °C (Table 3, Fig. 5). Similar to POM and DRM when the temperature increases from 600 to 800 °C, the process indicators increase (X_{CH4}: 44→85%, Y_{H2}: 51→77%, Y_{CO}: 28→74%) but even at 850 °C they do not reach equilibrium

Table 3. The influence of temperature, contact time, linear feed rate and composition of the reaction mixture on the performance of the SRM reaction

Catalyst quantity, g	Contact time, s	Linear feed rate, cm/min	Temperature of reaction, °C	Reaction indicators				
				X_{CH4}	Y_{CO2}	Y_{H2}	Y_{CO}	H_2/CO
$CH_4 : H_2O : He = 1 : 1.1 : 2.9$								
0.125	0.04	160	600	33	13	47	23	6.5
			700	63	7	63	50	4.1
			800	83	13	84	80	3.4
0.250	0.08	160	600	44	16	52	29	6.0
			700	77	11	75	62	4.0
			800	86	2	80	78	3.3
0.500	0.15	160	600	44	15	51	28	5.8
			700	72	10	72	60	3.8
			800	85	2	77	74	3.3
0.125	0.15	40	600	43	4	39	27	4.6
			700	65	0	56	41	4.3
			800	81	0	70	62	3.6
0.250	0.15	80	600	34	5	41	28	4.8
			700	64	0	59	51	3.9
			800	86	0	77	80	3.2
0.750	0.15	240	600	41	13	50	28	5.7
			700	79	10	81	65	3.9
			800	96	8	93	85	3.4
$CH_4 : H_2O : He = 1 : 0.8 : 3.2$								
0.500	0.15	160	600	38	7	47	32	4.5
			700	56	1	61	47	3.9
			800	72	0	70	53	4.0
$CH_4 : H_2O : He = 1 : 2.0 : 2.0$								
0.500	0.15	160	600	43	17	38	27	6.2
			700	83	26	61	53	5.0
			800	95	25	64	64	4.4

(Fig. 4). At the same time, a decrease in the H_2/CO ratio (5.8→3.3) and the yield of CO_2 by-product (15→2%) is observed. The high H_2/CO molar ratio and significant yield of CO_2 by-product at 600–700 °C are connected with the high impact of the water gas shift reaction (7) in this temperature range.

$$CO + H_2O \leftrightarrow CO_2 + H_2 \quad (7)$$

The change in process indicators when varying the contact time (0.04–0.15 s) and the linear feed rate of the reaction mixture (40–240 cm/min) is non-linear – first they increase, and then reach plateau. It has been established that when the molar ratio of the components $CH_4 : H_2O : He$ changes within the range of 1 : (0.8–2.0) : (2.0–3.2), the optimal process performance is achieved at a value of 1 : 1.1 : 2.9. A decrease in CH_4/H_2O leads to a significant increase in the CO_2 yield (0→25%) and the H_2/CO molar ratio (4.0→4.4) due to the increased contribution of the CO conversion reaction with steam.

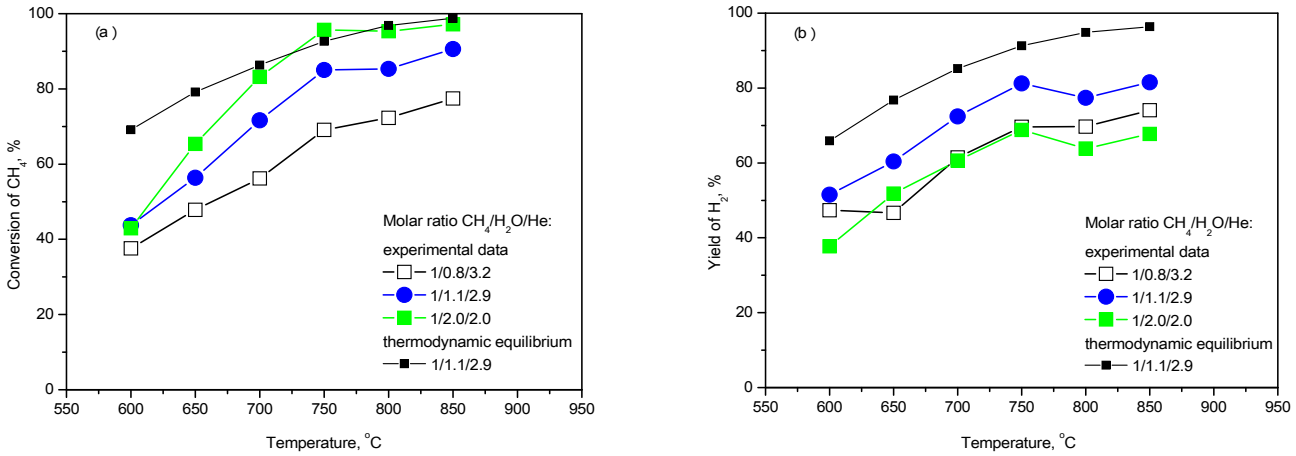

Fig. 5. Temperature dependence of methane conversion (a) and hydrogen yield (b) in the SRM reaction at different molar ratios of reagents.

3.4. Catalyst coking

It is known that in methane reforming processes, side reactions occur, which result in the formation of carbon deposits [18]. To study the contribution of such side processes in POM, DRM and SRM reactions, the degree of carbonization of the catalysts was determined. For this purpose, catalysts after the testing were studied by thermal analysis (Fig. 6, Table 4). It has been established that when air interacts with spent $Ce_{0.2}Ni_{0.8}O_{1.2}/Al_2O_3$ catalyst at elevated temperatures, a number of processes occur:

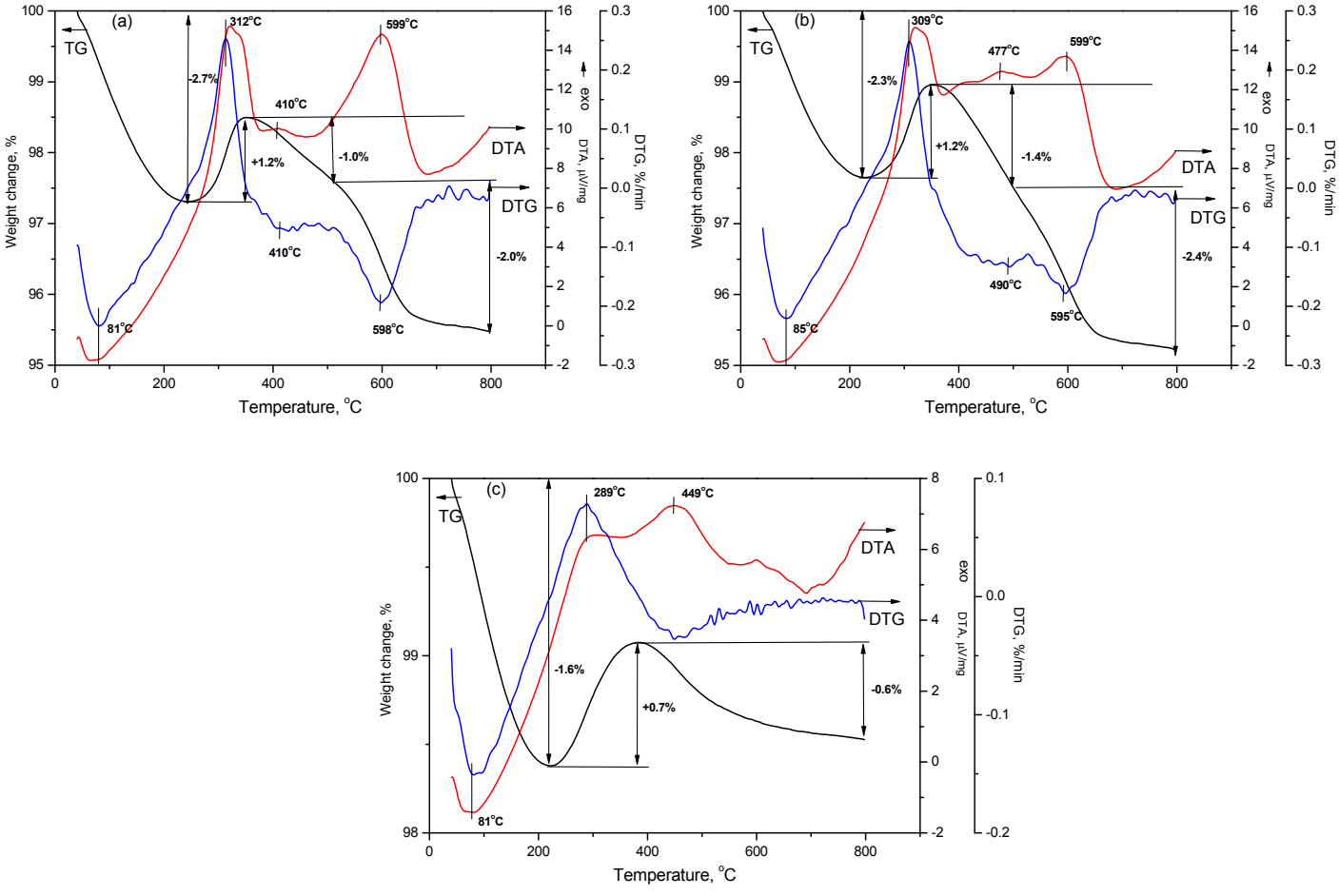

Fig. 6. Thermal analysis data for $Ce_{0.2}Ni_{0.8}O_{1.2}/Al_2O_3$ catalyst after testing in POM (a), DRM (b) and SRM (c) reactions. (a) – $CH_4 : O_2 : He = 1.0 : 0.5 : 3.5$, (b) – $CH_4 : CO_2 : He = 1.0 : 1.0 : 3.0$, (c) – $CH_4 : H_2O : He = 1 : 1.1 : 2.9$.

Table 4. Thermal analysis data for $Ce_{0.2}Ni_{0.8}O_{1.2}/Al_2O_3$ catalysts after testing in POM, DRM and SRM reactions and the degree of their carbonization (DC)

Molar ratio	Thermal analysis data						DC, %
	T_{DTG1}, °C (Δ_{m1}, %)	T_{DTG2}, °C (Δ_{m2}, %)	T_{DTG3}, °C (Δ_{m3}, %)	T_{DTA1}, °C	T_{DTA2}, °C	T_{DTA3}, °C	
			POM				
CH_4:O_2 = 1.0:0.5	81 (-2.7)	313 (+1.2)	410 (-1.0) 598 (-2.0)	65 endo	320 exo	410 exo 599 exo	3.0
CH_4:O_2 = 1.0:0.6	80 (-2.7)	314 (+1.3)	410 (-0.6) 588 (-0.9)	66 endo	322 exo	407 exo 583 exo	1.5
CH_4:O_2 = 1.0:0.7	86 (-2.5)	314 (+1.3)	425 (-0.6) 583 (-0.9)	69 endo	323 exo	410 exo 575 exo	1.5
			DRM				
CH_4:CO_2 = 1.0:0.8	89 (-1.5)	330 (+0.4)	489 (-15.1) 599 (-5.6)	-	330 exo	487 exo 609 exo	20.7
CH_4:CO_2 = 1.0:1.0	85 (-2.3)	309 (+1.2)	490 (-1.4) 595 (-2.4)	84 endo	320 exo	477 exo 595 exo	3.8
CH_4:CO_2 = 1.0:1.2	94 (-1.9)	315 (+1.4)	(-1.7)	75 endo	336 exo	411 exo 575 exo	1.7
CH_4:CO_2 = 1.0:1.4	79 (-2.4)	313 (+1.4)	424 (-1.3) 590 (-0.9)	65 endo	334 exo	406 exo 573 exo	2.2
			SRM				
CH_4:H_2O = 1.0:0.8	86 (-1.6)	315 (+0.3)	482 (-15.2)	-	269 exo	480 exo	15.2
CH_4:H_2O = 1.0:1.1	81 (-1.6)	289 (+0.7)	449 (-0.6)	81 endo	287 exo	449 exo	0.6
CH_4:H_2O = 1.0:2.0	85 (-1.9)	286 (+0.7)	(-0.4)	85 endo	293 exo	464 exo	0.4

1) desorption of water (75 °C < T_{DTG1} < 100 °C), accompanied by loss of sample weight (Δ_{m1} = 2±1%) and an endothermic effect (60 °C < T_{DTA1} < 90 °C);

2) oxidation of the nickel-containing active component (280 °C < T_{DTG2} < 340 °C), accompanied by an increase in sample weight (Δ_{m2} = 0.4–1.4%) and an exothermic effect (265 °C < T_{DTA2} < 340 °C);

3) oxidation of carbon deposits (400 °C < T_{DTG3} < 600 °C), accompanied by loss of sample weight (Δ_{m3} = 0.4–20.7%) and one or two exothermic effects (400 °C < T_{DTA3} < 610 °C).

The weight loss of the sample in the temperature range 400–900 °C, caused by the oxidation of carbon-containing components of the sample, corresponded to the degree of sample carbonization (DC).

It has been established that the amount and temperature of burnout of carbon deposits, which characterizes the degree of their condensation, depend on the conditions of the catalytic reaction (Table 4). The resistance of catalysts to carbonization increases with increasing O/C molar ratio in the initial reaction mixture. In particular, the degree of their carbonization decreases from 3 to 1.5% for POM, from 20.7 to 2.2% for DRM, and from 15.2 to 0.4% for SRM. The high degree of carbonization of the studied samples at the ratios CH_4:CO_2 = 1.0:0.8 and CH_4:H_2O = 1.0:0.8 is associated with a low O/C molar ratio of 0.8. When O/C < 1, because of a lack of oxygen, along with the target reactions, a side process of carbon formation occurs to a large extent due to the reaction (6).

3.5. Influence of conditions on process efficiency

The study of POM, DRM, and SRM reactions in the presence of a $Ce_{0.2}Ni_{0.8}O_{1.2}/Al_2O_3$ catalyst showed that in optimal reaction conditions a high yield of hydrogen is achieved with a sufficiently high conversion of the reagents. The optimal conditions are similar for all reactions studied: temperature – 800–850 °C, contact time – 0.15 s, and linear speed – 160 cm/min. At 800 °C, the highest hydrogen yield

(more than 95%) with a reagent conversion of more than 90% was obtained in the POM and DRM reactions. Slightly lower figures in the case of the SRM reaction, where the hydrogen yield was 77% with a methane conversion of 85%. However, the processes are close in hydrogen concentration, providing 30±5 vol.%. The molar ratio increases in a series of reactions DRM < POM < SRM, amounting to 1.0, 2.3, and 3.3 respectively. The obtained hydrogen yield is comparable to or higher than those described in the literature [19–21]. The high activity of the $Ce_{0.2}Ni_{0.8}O_{1.2}/Al_2O_3$ catalyst in all three processes will allow it to be successfully used for tri-reforming coal mine methane of different compositions. However, before widespread industrial use, it is necessary to ensure the stability and regenerability of this catalyst, which is the subject of our further research.

In terms of resistance to carbonization, the processes are arranged in a row: DRM < POM < SRM. This is due to the dependence of the amount of carbon deposits on the molar ratio of O/C in the initial reaction mixture and is consistent with the results of thermodynamic calculations [14]. It can be seen that the maximum yield of hydrogen with a small amount of carbon deposits is provided at an O/C molar ratio of 1.1–1.2 (Fig. 7). In this case, the degree of carbonization is less than 3%, which is a good result for reforming processes [15, 22–25]. Lower values of this parameter lead to a sharp increase in coking, and higher values lead to an increase in the yield of the undesirable product – CO_2. Accordingly, to increase the resistance of catalysts to deactivation, it is necessary to purposefully regulate the O/C molar ratio in the initial reaction mixture by adding oxidizing reagents (H_2O, CO_2) to the coal mine methane.

Table 5 shows the results of research reported in recent literature concerning Ni based catalysts for POM, DRM and SRM reactions. $Ce_{0.2}Ni_{0.8}O_{1.2}/Al_2O_3$ has comparable to or higher performance than those described in the literature [15, 19–25]. As it was mentioned above, in this material, aluminum oxide provides thermal stability of the catalyst; cerium dioxide serves as an oxygen buffer and plays a role in the activation of oxygen-containing molecules, and nickel is highly active in activating methane. The sol-gel preparation method used ensures high dispersion of the Ni active component and an extended metal-cerium dioxide interface, which increases the number of active centers and their resistance to sintering and coking.

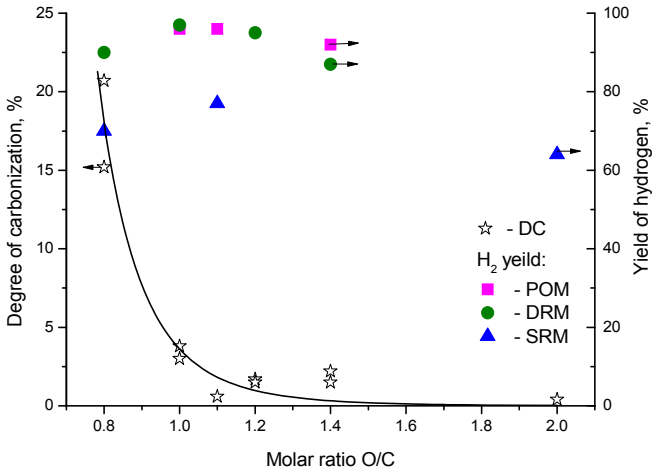

Fig. 7. Influence of O/C molar ratio on the degree of catalyst carbonization and yield of hydrogen in POM, DRM and SRM reactions.

5. Conclusions

The behavior of the target reactions that make up the tri-reforming process was studied when operating conditions varied over a wide range. The temperature dependences of the process indicators (methane conversion, hydrogen yield) were determined. Optimal reaction conditions were elucidated to ensure maximum efficiency of hydrogen production by reforming methane-containing mixtures of various compositions (temperature in the range 800–850 °C, contact time 0.15 s, linear feed rate 160 cm/min, molar ratio of CH_4:O_2 = 1:0.5 for POM, CH_4:CO_2 = 1:1 for DRM, CH_4:H_2O = 1:1.1 for SRM). H_2/CO control was achieved over a wide range (0.9–6.5). It is demonstrated that the maximum yield of hydrogen with a small amount of carbon deposits is provided at an O/C molar ratio of 1.1–1.2. The hydrogen concentration in the resulting hydrogen-containing mixture is determined by the type of process and is equal to 30±5 vol.%. The high activity of the $Ce_{0.2}Ni_{0.8}O_{1.2}/Al_2O_3$ catalyst in various reforming processes allows us to recommend it for the processing of coal mine methane by the tri-reforming method.

Funding

The investigation was carried out with support from the Russian Science Foundation under Project No. 22-13-20040, https://rscf.ru/project/22-13-20040/» and from the Region – the Kemerovo Region – Kuzbass.

Table 5. Performance of Ni based catalysts in the reforming of methane

Catalysts	Reaction conditions	Performance	Content of coke, wt. %	Reference
		POM		
$Ce_{0.2}Ni_{0.8}O_{1.2}/Al_2O_3$	$CH_4 : O_2 : N_2 = 1 : 0.5 : 3.5$, T = 700 °C	X_{CH4} = 85%, Y_{H2} = 86%	3.0	This work
Ni/Al_2O_3	$CH_4 : O_2 : He = 1 : 0.5 : 1.9$, T = 750 °C	X_{CH4} = 80%, Y_{H2} = 80%	The formation of different types of carbon	[26]
Ni/Al_2O_3	$CH_4 : O_2 : N_2 = 1 : 0.5 : 5$, T = 700 °C	X_{CH4} = 78%	No data	[27]
$Ni/CeO_2/Al_2O_3$	$CH_4 : O_2 : N_2 = 1 : 0.5 : 5$, T = 700 °C	X_{CH4} = 80%	No data	[27]
		DRM		
$Ce_{0.2}Ni_{0.8}O_{1.2}/Al_2O_3$	$CH_4 : CO_2 : He = 1 : 1 : 3$, T = 700 °C	X_{CH4} = 79%, Y_{H2} = 82%	3.8	This work
Ni/Al_2O_3	$CH_4 : CO_2 : N_2 = 1 : 1 : 6$, T = 700 °C	X_{CH4} = 44%	6.9	[27]
$Ni/CeO_2/Al_2O_3$	$CH_4 : CO_2 : N_2 = 1 : 1 : 6$, T = 700 °C	X_{CH4} = 60%	2.1	[27]
$Ni/MgO/Al_2O_3$	$CH_4 : CO_2 : N_2 = 49 : 49 : 2$, T = 750 °C	X_{CH4} = 60%	37.5	[28]
		SRM		
$Ce_{0.2}Ni_{0.8}O_{1.2}/Al_2O_3$	$CH_4 : H_2O : He = 1 : 1.1 : 2.9$, T = 700 °C	X_{CH4} = 72%, Y_{H2} = 72%	0.6	This work
Ni/Al_2O_3	$CH_4 : H_2O : N_2 = 1 : 1 : 5$, T = 700 °C	X_{CH4} = 47%	No data	[27]
$Ni/CeO_2/Al_2O_3$	$CH_4 : H_2O : N_2 = 1 : 1 : 5$, T = 700 °C	X_{CH4} = 47%	No data	[27]
$Ni/CeO_2/Al_2O_3$	$CH_4 : H_2O : N_2 = 1 : 3 : 3$, T = 700 °C	X_{CH4} = 70%, Y_{H2} = 60%	No data	[29]

Acknowledgments

The authors are grateful to O.B. Sukhova for help with catalyst characterization.

References

[1]. Statistical Review of World Energy 2023. https://www.energyinst.org/__data/assets/pdf_file/0004/1055542/EI_Stat_Review_PDF_single_3.pdf

[2]. Global thermal coal 10-year investment horizon outlook 2023. https://www.woodmac.com/reports/coal-global-thermal-coal-10-year-investment-horizon-outlook-2023-150177005/

[3]. Global Methane Tracker 2023. IEA. https://www.iea.org/reports/global-methane-tracker-2023

[4]. Coal 2023. IEA. https://iea.blob.core.windows.net/assets/a72a7ffa-c5f2-4ed8-a2bf-eb035931d95c/Coal_2023.pdf

[5]. 2006 IPCC Guidelines for National Greenhouse Gas Inventories. Vol. 2. Energy, Chapter 4: Fugitive Emissions. https://www.ipcc-nggip.iges.or.jp/public/2006gl/pdf/2_Volume2/V2_4_Ch4_Fugitive_Emissions.pdf

[6]. Driving Down Coal Mine Methane Emissions. IEA. https://iea.blob.core.windows.net/assets/ab2115cd-2b04-4e66-9a71-ec2c14d13acf/DrivingDownCoalMineMethaneEmissions.pdf

[7]. Coal mine methane emissions and methane intensity of production in selected countries 2022. https://www.iea.org/data-and-statistics/charts/coal-mine-methane-emissions-and-methane-intensity-of-production-in-selected-countries-2022

[8]. D.S.S.S. Sirigina, A. Goel, S.M. Nazir, *Sci. Rep.* 13 (2023) 1–15. DOI: 10.1038/s41598-023-44582-w

[9]. J. Yin, S. Su, J.S. Bae, X.X. Yu, M. Cunnington, Y. Jin, *Energy Fuels* 34 (2020) 655–664. DOI: 10.1021/acs.energyfuels.9b03076

[10]. K. Wei, X. Wang, H. Zhu, H. Liu, S. Wang, F. Chen, F. Zhou, Y. Ling, *J. Power Sources* 506 (2021) 230208. DOI: 10.1016/j.jpowsour.2021.230208
[11]. H. Zhu, H. Dai, Z. Song, X. Wang, Z. Wang, H. Dai, S. He, *Int. J. Hydrogen Energy* 46 (2021) 31439–31451. DOI: 10.1016/j.ijhydene.2021.07.036
[12]. E.V. Matus, I.Z. Ismagilov, E.S. Mikhaylova, Z.R. Ismagilov, *Eurasian Chem.-Technol. J*. 24 (2022) 69–91. DOI:10.18321/ectj1320
[13]. A.P. Nikitin, S.A. Sozinov, E.V. Matus, Z.R. Ismagilov, *Chem. Sustain, Develop*. 31 (2023) 552–560. DOI: 10.15372/CSD2023500
[14]. E.V. Matus, Z.R. Ismagilov, *Eurasian Chem.-Technol. J.* 24 (2022) 203–214. DOI: 10.18321/ectj1433
[15]. R.D. Alli, P.A.L. de Souza, M. Mohamedali, L.D. Virla, N. Mahinpey, *Catal. Today* 407 (2023) 107–124. DOI: 10.1016/j.cattod.2022.02.006
[16]. E.V. Matus, M.A. Kerzhentsev, A.P. Nikitin, S.A. Sozinov, Z.R. Ismagilov, *Eurasian Chem.-Technol. J.* 25 (2023) 103–113. DOI: 10.18321/ectj1500
[17]. E. Matus, M. Kerzhentsev, I. Ismagilov, A. Nikitin, S. Sozinov, Z. Ismagilov, *Energies* 16 (2023) 2993. DOI: 10.3390/en16072993
[18]. S. Arora, R. Prasad, *RSC Adv.* 6 (2016) 108668–108688. DOI: 10.1039/c6ra20450c
[19]. R. Kumar, K.K. Pant, *Fuel Process. Technol.* 210 (2020) 106559. DOI: 10.1016/j.fuproc.2020.106559
[20]. M. Schmal, F.S. Toniolo, C.E. Kozonoe, *Appl. Catal. A Gen.* 568 (2018) 23–42. DOI: 10.1016/j.apcata.2018.09.017
[21]. D. Pham Minh, X.H. Pham, T.J. Siang, D.V.N. Vo, *Appl. Catal. A Gen.* 621 (2021) 118202. DOI: 10.1016/j.apcata.2021.118202
[22]. P. Li, Y.H. Park, D.J. Moon, N.C. Park, Y.C. Kim, *J. Nanosci. Nanotechnol.* 16 (2016) 1562–1566. DOI: 10.1166/jnn.2016.12006
[23]. T.J. Siang, T.L.M. Pham, N. Van Cuong, et al., *Microporous Mesoporous Mater.* 262 (2018) 122–132. DOI: 10.1016/j.micromeso.2017.11.028
[24]. Z. Zhao, P. Ren, W. Li, B. Miao, *Int. J. Hydrogen Energy* 42 (2017) 6598–6609. DOI: 10.1016/j.ijhydene.2016.11.144
[25]. I. Wysocka, A. Mielewczyk-Gryń, M. Łapiński, B. Cieślik, A. Rogala, *Int. J. Hydrogen Energy* 46 (2021) 3847–3864. DOI: 10.1016/j.ijhydene.2020.10.189
[26]. C. Alvarez-Galvan, M. Melian, L. Ruiz-Matas, J.L. Eslava, R.M. Navarro, M. Ahmadi, B. Roldan Cuenya, J.L.G. Fierro, *Front. Chem.* 7 (2019) Art. 104. DOI: 10.3389/fchem.2019.00104
[27]. F. Pompeo, D. Gazzoli, N.N. Nichio, *Int. J. Hydrogen Energy* 34 (2009) 2260–2268. DOI: 10.1016/j.ijhydene.2008.12.057
[28]. L. Zhang, Q. Zhang, Y. Liu, Y. Zhang, *Appl. Surf. Sci.* 389 (2016) 25–33. DOI: 10.1016/j.apsusc.2016.07.063
[29]. Y. Khani, F. Bahadoran, Z. Shariatinia, M. Varmazyari, N. Safari, *Ceram. Int.* 46 (2020) 25122–25135. DOI: 10.1016/j.ceramint.2020.06.299